Environmental Science & Technology

pubs.acs.org/est

Article

Probing Long-Term Impacts: Low-Dose Polystyrene Nanoplastics Exacerbate Mitochondrial Health and Evoke Secondary Glycolysis via Repeated and Single Dosing

Miao Peng, Charlotte Grootaert, Maaike Vercauteren, Nico Boon, Colin Janssen, Andreja Rajkovic,*,⊥ and Jana Asselman⊥

Cite This: *Environ. Sci. Technol.* 2024, 58, 9967−9979

Read Online

ACCESS | Metrics & More | Article Recommendations | Supporting Information

ABSTRACT: Nanoplastics (NPs) are omnipresent in the environment and contribute to human exposure. However, little is known regarding the long-term effects of NPs on human health. In this study, human intestinal Caco-2 cells were exposed to polystyrene nanoplastics (nanoPS) in an environmentally relevant concentration range (10^2−10^9 particles/mL) under two realistic exposure scenarios. In the first scenario, cells were repeatedly exposed to nanoPS every 2 days for 12 days to study the long-term effects. In the second scenario, only nanoPS was added once and Caco-2 cells were cultured for 12 days to study the duration of the initial effects of NPs. Under repeated dosing, initial subtle effects on mitochondria induced by low concentrations would accrue over consistent exposure to nanoPS and finally lead to significant impairment of mitochondrial respiration, mitochondrial mass, and cell differentiation process at the end of prolonged exposure, accompanied by significantly increased glycolysis over the whole exposure period. Single dosing of nanoPS elicited transient effects on mitochondrial and glycolytic functions, as well as increased reactive oxygen species (ROS) production in the early phase of exposure, but the self-recovery capacity of cells mitigated these effects at intermediate culture times. Notably, secondary effects on glycolysis and ROS production were observed during the late culture period, while the cell differentiation process and mitochondrial mass were not affected at the end. These long-term effects are of crucial importance for comprehensively evaluating the health hazards arising from lifetime exposure to NPs, complementing the extensively observed acute effects associated with prevalent short-term exposure to high concentrations. Our study underlines the need to study the toxicity of NPs in realistic long-term exposure scenarios such as repeated dosing.

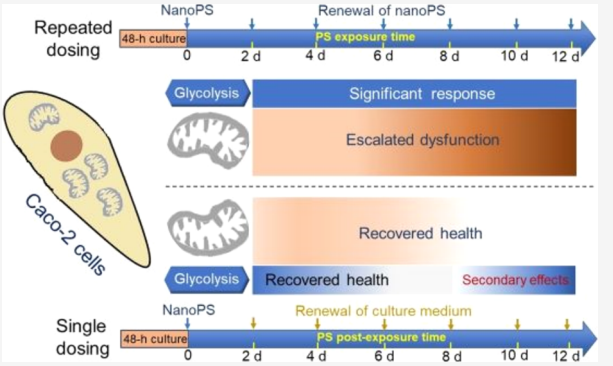

KEYWORDS: *cell differentiation, glycolysis, long-term effects, mitochondrial mass, mitochondrial respiration*

1. INTRODUCTION

Presently, an increasing number of studies have highlighted that daily plastic products can release trillions of nanoplastics (NPs), referring to plastic particles with dimensions smaller than 1000 nm, during regular use such as the food preparation processes.[1−4] At the same time, plastic particles are increasingly detected in various food and water matrices.[5−7] Collectively, these findings suggest that individuals are consistently exposed to nanoplastics via the consumption of food and beverages throughout their entire lifespan. Dietary exposure to NPs is influenced by their prevalence in various commodities and specific dosing patterns. However, currently, the majority of studies focus on acute in vitro effects of single dosing of micro- or nanoplastics at relatively high levels.[8−11]

Studies on long-term exposure to NPs are likely to represent a more realistic scenario than the current acute toxicity models, potentially inducing subchronic cell dysfunction that may impact development, growth, and body homeostasis, as well as contribute to the onset, severity, or progression of chronic diseases as a consequence of lifetime exposure (especially for vulnerable populations).[12,13] Furthermore, the duration of the effects of NPs subsequent to initial uptake may differ from what has been extensively reported in previous short-term studies with in vitro human cell lines due to the dynamic equilibrium between internalization and excretion of NPs from cells, cell homeostasis, proliferation, and differentiation. The carefully calibrated exposure duration will also reflect the role of potential hormesis. Despite their potential relevance to actual health

Received: December 23, 2023
Revised: May 22, 2024
Accepted: May 23, 2024
Published: May 30, 2024

effects, long-term exposure to NPs remains largely uncharacterized.

Mitochondria play a central role in many diseases and are exposed for various reasons, as they are responsible for producing adenosine triphosphate (ATP) via oxidative phosphorylation, which is a key metabolic energy pathway moderated by oxygen (O_2) consumption. Glycolysis is another basic metabolic pathway to produce ATP occurring at low O_2 flux conditions, which can compensate for mitochondrial respiration and regulate blood glucose levels to prevent hyperglycemia (high blood sugar) or hypoglycemia (low blood sugar).[14−16] Our previous investigation demonstrated that single dosing of microplastics at low doses (10^2−10^5 particles/mL) led to increased mitochondrial respiration and reactive oxygen species (ROS) production in Caco-2 cells after 12 days postexposure.[17] Moreover, both our previous research and other studies have identified significant effects of nanoplastics on mitochondrial respiration and glycolysis as well as metabolic shift between energy phenotypes for short-term exposure (a few hours after exposure, corresponding to acute effects).[18−20] These findings together indicate that long-term exposure to NPs, referring to a few days, weeks, or years after exposure (corresponding to long-term effects), has the potential to impact both mitochondrial and glycolytic functions. Furthermore, mitochondrial respiration and glycolysis provide the energy required for cell differentiation and mitochondria to undergo fission and fusion during differentiation.[21−24] Thus, molecular crosstalk and mutual influence exist among mitochondrial respiration, glycolysis, and differentiation, creating a complex interplay in cellular physiology. Simultaneously, these endpoints serve as optimal indicators for investigating the long-term effects of NPs on human cells.

By measuring the appropriate endpoints mentioned in prolonged exposure, this study explored cytotoxicity, oxidative stress, bioenergetics, and cell differentiation in repeated versus single-dosing long-term exposures to address the current knowledge gaps. To this end, Caco-2 cells, a human intestinal epithelial model representing the ingestion pathway, were exposed to nanoPS at an environmentally relevant concentration range (10^2−10^9 particles/mL, Table S1) under two different scenarios: (i) nanoPS was repeatedly added to cells every 2 days for 12 days to study the long-term effects, and (ii) nanoPS was added to cells once and then further cultured for 12 days to study the duration of the effects of NPs. Mitochondrial activity, oxidative stress (ROS production), mitochondrial respiration, glycolysis, mitochondrial mass, and cell differentiation markers were regularly monitored over the two long-term periods. This early-stage research is a pioneering exploration into the toxicity of NPs under realistic long-term exposure scenarios, which could be of paramount significance in assessing the health risks associated with lifetime exposure to NPs.

2. MATERIALS AND METHODS

2.1. Cell Culture. The adenocarcinomic human epithelial colon cell line (Caco-2) was purchased from the American Type Culture Collection (ATCC, Manassas, VA) and kept under Biobank number BB190156. Caco-2 cells were grown in Dulbecco's modified Eagle's medium (DMEM) supplemented with phenol red, 100 U/mL penicillin, 100 μg/mL streptomycin, 10% fetal bovine serum (FBS), and 2% nonessential amino acids (NEAA). All cultures and supplemented solutions were obtained from Thermo Fisher Scientific. Caco-2 cells were cultured in an incubator under 5% CO_2 at 37 °C, and a relative humidity of 95% to 100%, and their growth and confluence were checked daily using light microscopy. Confluent cells were detached using 0.5% trypsin-EDTA (Thermo Fisher Scientific) once a week at a splitting ratio of 1:4. The Caco-2 cells used in this work had passage numbers of less than 30.

2.2. Nanoplastics (Polystyrene). The 100 nm polystyrene (PS) nanospheres (2.5% solids [w/v] in water) used in this study were purchased from Polysciences Inc. with stock solutions of 4.55×10^{13} particles/mL (P/mL). After ultrasonic treatment (5 min) and vortexing, the stock solution was serially diluted 100 times twice with culture medium (the same medium was used to culture cells) to obtain 4.55×10^9 P/mL, which was set as the highest tested concentration. Lower concentrations were derived from a dilution factor of 10 from the highest concentration (4.55×10^9 P/mL) in the culture medium. After dilutions, the expected exposure concentrations were 4.55×10^2, 4.55×10^3, 4.55×10^4, 4.55×10^5, 4.55×10^6, 4.55×10^7, 4.55×10^8, and 4.55×10^9 P/mL. The characterization of PS nanoplastics is described in Supporting File 2 of Supporting Information (SI), which includes the results from scanning electron microscopy and dynamic light scattering. In addition, the characterization and quantification of additives and leachates using gas chromatography-mass spectrometry (GC-MS) are provided in Supporting File 3 of SI.

2.3. In Vitro Exposure of Cells to PS Nanoplastics. Prior to the experiment, trypsinized Caco-2 cells were detached and suspended in the culture medium, as described above. First, the cell suspension was diluted and seeded in the following plates: (1) 96-well plates (20,000 cells per well with 200 μL of the medium) for the cellular assays (see below); (2) seahorse XFe96 microplates (8000 cells per well with 80 μL of the medium) for bioenergetic measurements (see below); (3) 6-well plates (300,000 cells per well with 3000 μL of the medium) for western blotting (see below); and (4) 24-well plates (100,000 cells per well with 1000 μL of the medium) for MitoTracker Green FM staining (see below). The seeding density of cells was selected based on the previous literature.[25] In this seeding density, cells were at least 80% confluent after 48 h of culture to guarantee that they were stable and robust before PS exposure.

As depicted in Figure 1, two exposure scenarios were applied to mimic the expected situations. In scenario 1 (S1), Caco-2

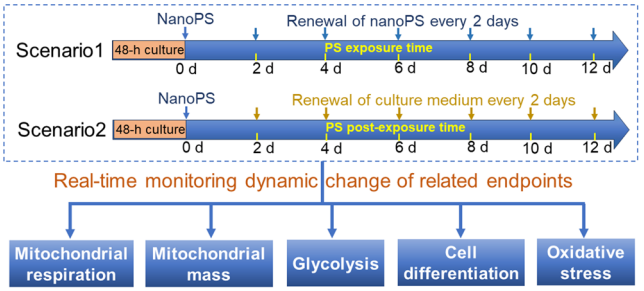

Figure 1. Schematic of experimental design employed in this study.

cells were repeatedly treated with nanoPS every 2 days for 12 days of exposure (6 exposures in total). For scenario 2 (S2), Caco-2 cells were exposed to single dosing of nanoPS for 2 days, followed by a 12-day culture period. As a result, the final concentration in the repeated dosing pattern was higher than that in the single-dosing version. As demonstrated in our previous studies,[17,25,26] Caco-2 cells exhibited a pronounced acidification tendency and subsequent detachment from the full-

https://doi.org/10.1021/acs.est.3c10868
Environ. Sci. Technol. 2024, 58, 9967−9979

bottom standard culture plates utilized in this study after 14 days of culture. Thus, in the two scenarios, a 12-day exposure was employed, supplemented with a 2-day culture period prior to exposure, resulting in a total experimental duration of 14 days. For all experiments, the culture medium was used as a negative control (blank), and the culture medium was changed every 48 h. Mitochondrial activity and oxidative stress were measured using biochemical MTT and ROS assays, respectively. The Agilent Seahorse XF Cell Mito Stress Test was performed to explore the mitochondrial function and energy metabolic pathways in more detail. Western blotting was performed to check the progress of cell differentiation during exposure. MitoTracker Green FM staining was used to evaluate mitochondrial mass during long-term exposure. Figure S6 of SI shows the overview of the measured endpoints at different timeslots.

2.4. Cellular and Biochemical Assays. *2.4.1. MTT (3-(4,5-Dimethylthiazol-2-yl)-2,5-diphenyltetrazolium bromide) Assay.* First, 100 μL of the cell culture medium was removed from each well. Next, 20 μL of MTT (5 mg/mL) was added to each well. The treated cells were incubated in the dark for 2 h at 37 °C. All media were then carefully removed, and 200 μL of pure DMSO was added to each well. DMSO was suspended several times to form a homogeneous purple solution. Finally, the absorbance of each well was measured at 570 nm with a Spectramax Gemini XS Fluorescence Plate Reader. Cells treated with 10% DMSO were used as positive controls, and each treatment had six replicates.

2.4.2. Intracellular Reactive Oxygen Species (ROS) Assay. First, the exposure medium was removed, and 20 μM H_2-DCFDA (2,7-dichlorodihydrofluoresceindiacetate) in 200 μL of DMEM without phenol red was added. After incubation in the dark for 20 min at 37 °C, the medium was replaced with 200 μL of phenol red-free DMEM. Finally, the fluorescence of the stained cells was measured using a Spectramax Gemini XS Fluorescence Plate Reader with excitation and emission wavelengths of 485 and 535 nm, respectively. Cells treated with 10% DMSO were used as positive controls, and each treatment had six replicates.

2.5. Bioenergetic Profiles. Seahorse experiments were conducted at time points of 2, 4, 8, 10, and 12 days for both scenarios 1 and 2. Prior to the XF assay, the Seahorse XF Sensor Cartridge was loaded with 180 μL of Seahorse XF Calibrant Solution, and incubated overnight at 37 °C without CO_2 according to the manufacturer's instructions. Before analysis, Caco-2 cells were washed twice with the XF Assay Medium (Agilent Seahorse Bioscience, Santa Clara, CA) with the addition of 1 mM pyruvate, 10 mM glucose, and 2 mM glutamine and incubated at 37 °C without CO_2 for 45 min. Then, the Caco-2 cells were subjected to an Agilent Seahorse Cell Mito Stress Test via a sequential injection of oligomycin (OM) (1 μM for 2 and 4 days exposure, 1.5 μM for 8 days exposure, 2 μM for 10 and 12 days exposure), Carbonyl cyanide-4-(trifluoromethoxy) phenylhydrazone (FCCP) (0.5 μM for 2 and 4 days exposure, 1 μM for 8 days exposure, 2 μM for 10 and 12 days exposure) and a mixture of rotenone and antimycin A (ROT/AA) (0.5 μM). The extracellular acidification rate (ECAR) and oxygen consumption rate (OCR) were measured using an Agilent Seahorse XFe96 extracellular flux analyzer (Agilent Seahorse Bioscience, Santa Clara, CA) according to the manufacturer's instructions. The calculation of mitochondrial respiration parameters, glycolytic parameters, and ATP production rate was described in detail in our previous paper.[18] The bioenergetic health index (BHI) was calculated using the following formula: BHI = (ATP-linked respiration × spare respiratory capacity)/(proton leak × nonmitochondrial respiration).[27,28] These four input parameters were obtained from the seahorse analyzer during the Cell Mito Stress Test.

2.6. Western Blotting. Western blotting analysis was performed to identify the specific protein markers related to Caco-2 cell differentiation. In this study, Western blotting was conducted after 4 and 12 days of exposure in scenarios 1 and 2, respectively, with three concentrations of nanoPS (10^3, 10^6, and 10^9 P/mL). First, the cell medium was aspirated from the 6-well plates, and then the cells were washed with cold phosphate-buffered saline (PBS). The washed cells were lysed in Laemmli buffer, and the cell suspension was transferred to Eppendorf tubes. Next, the collected cells were sonicated and vortexed to disrupt the cell membranes and release the proteins. The cells were protected on ice during all incubation steps to avoid protein degradation. The disrupted cells were centrifuged at 12000 rpm for 10 min, and the supernatants were used to quantify the total protein content. After quantification and denaturation, the protein samples were separated on a 10% sodium dodecyl sulfate-polyacrylamide gel and transferred onto nitrocellulose membranes (Millipore). After blocking, the membranes were incubated with primary antibodies, rinsed, and then incubated with secondary antibodies. Images of the protein signals on the membranes were acquired using a ChemiDoc MP (Biorad) imaging system. The relative expressions of proteins were analyzed using Image Lab software (version 6.0.1). The primary antibodies included ZO-1 monoclonal antibody (ZO-1−1A12; molecular weight: 210 kDa), occludin monoclonal antibody (OC-3F10; molecular weight: 65 kDa), villin polyclonal antibody (molecular weight: 92 kDa), claudin-1 polyclonal antibody (MH25; molecular weight: 20 kDa); and β-tubulin polyclonal antibody (molecular weight: 55 kDa). Secondary antibodies were anti-rabbit IgG (H + L) and anti-mouse IgG (H + L) cross-adsorbed secondary antibodies.

2.7. Mitochondria Staining. After exposure, the Caco-2 cells were washed with PBS and detached using 0.5% trypsin-EDTA. The detached cells were then stained with MitoTracker Green FM (Thermo Fisher Scientific) at a dilution of 1000 times for 20 min at 37 °C. Next, the fluorescence of the stained mitochondria was measured using an Attune NxT flow cytometer equipped with a blue laser (488 nm) for excitation and a 530 nm emission filter. The mitochondrial mass was detected by a gating strategy based on sideward scatter and green fluorescence in the blue laser channel (see Figure S7 in Supporting Information), as reported by related literature.[29,30]

2.8. Statistical Analysis. All data were normalized to the negative control (untreated cells) (=100%). Statistical analysis was performed using one-way analysis of variance (ANOVA), or nonparametric Kruskal−Wallis test with Tukey's post-hoc test using R-studio. Statistical significance was indicated by $*p \leq 0.05$. A positive control was used for quality assurance of the performed assays. Time−response curves of mitochondrial parameters were fitted via drc package (LL4 model) using R-studio.[31]

3. RESULTS

3.1. Variable Mitochondrial Activity and ROS over Long-Term Exposure. In scenario 1 (S1) with repeated PS exposure, mitochondrial activity showed significant loss at all tested PS concentrations in the early timeslot (Figures S8A and

https://doi.org/10.1021/acs.est.3c10868
Environ. Sci. Technol. 2024, 58, 9967−9979

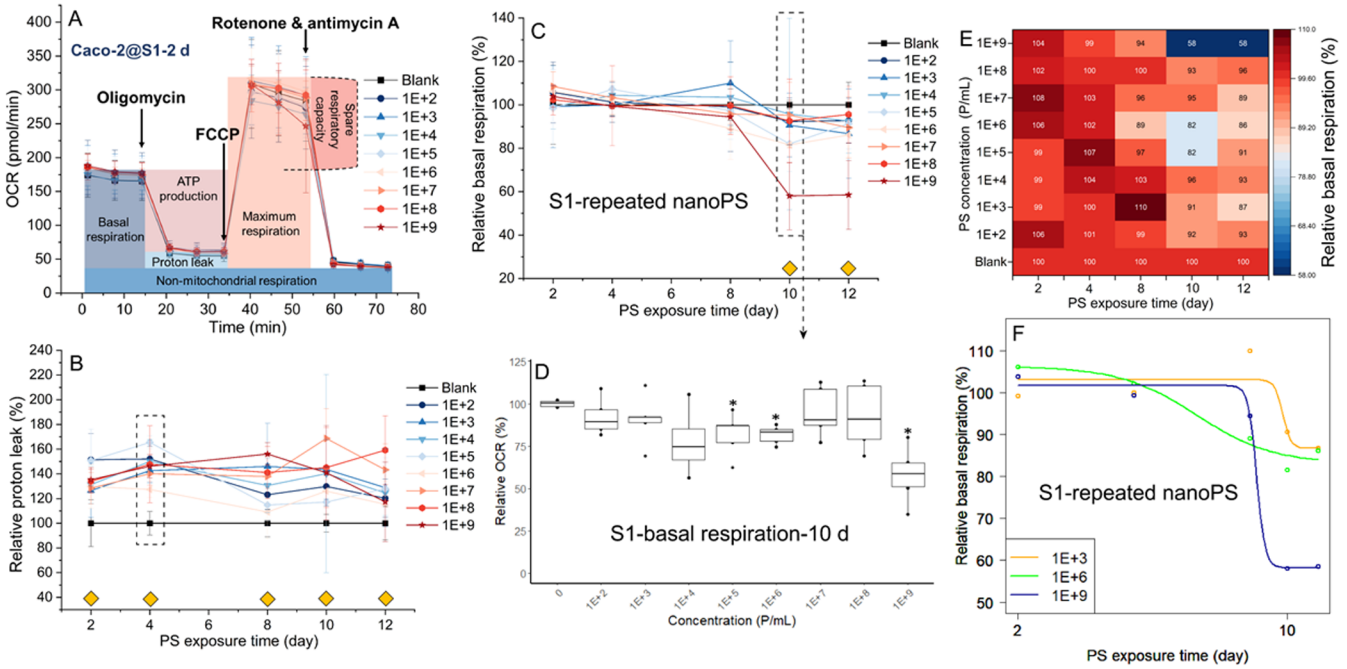

Figure 2. (A) Mitochondrial profiles of nanoPS-treated Caco-2 cells in response to the consecutive addition of pharmacological stressors of the mitochondrial electron transport in scenario 1 (S1) after 2 days. (B) Relative proton leak of Caco-2 cells exposed to repeated nanoPS in S1 over exposure time (see details of the time point with a dashed rectangle in Figure S5B). (C) Relative basal respiration of Caco-2 cells exposed to repeated nanoPS and (E) the heatmap with corresponding mean values of each treatment in S1 over exposure time. (D) Relative oxygen consumption rate (OCR) from basal respiration of Caco-2 cells exposed to different concentrations of nanoPS after 10 days of exposure in S1. (F) Fitted time−response curves of relative basal respiration of Caco-2 cells exposed to three representative concentrations (10^3, 10^6, and 10^9 P/mL) in S1 over exposure time. Caco-2 cells in the culture medium were used as a negative control (100%); $n = 5$. *$p \leq 0.05$, a significant difference compared to the negative control. Yellow squares indicate the statistical significance of at least one nanoPS concentration at specific time points.

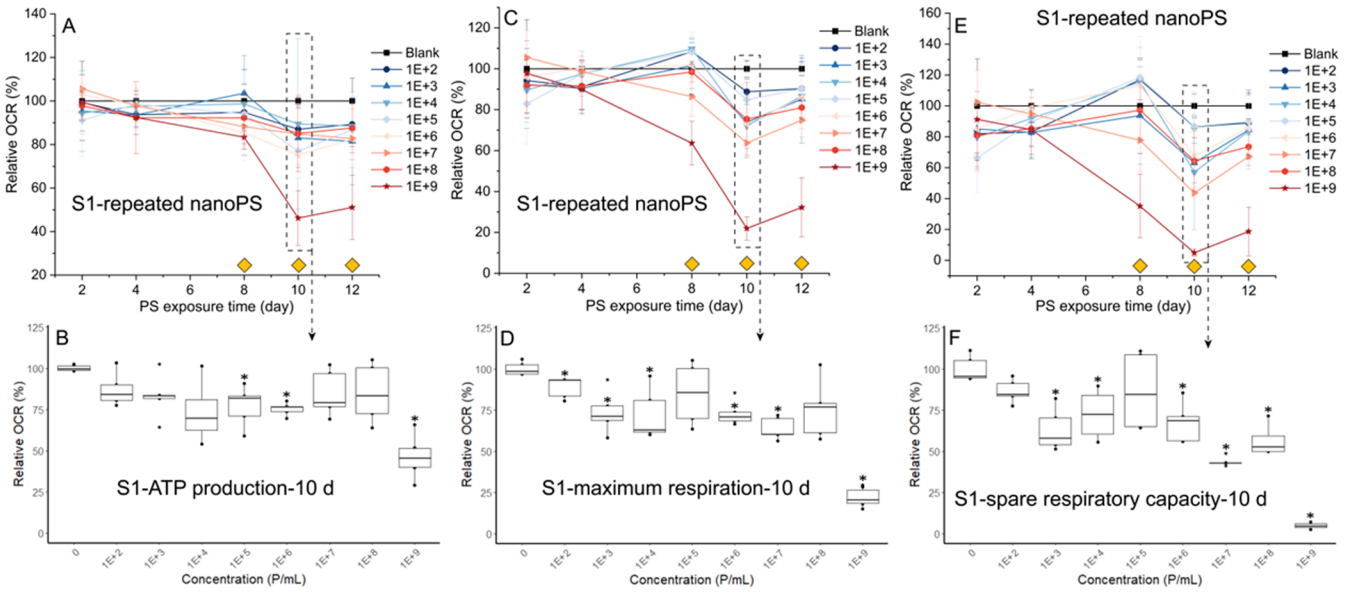

Figure 3. (A) Relative ATP production in Caco-2 cells exposed to repeated nanoPS in scenario 1 (S1) over exposure time. (B) Relative oxygen consumption rate (OCR) from ATP production of Caco-2 cells exposed to different concentrations of nanoPS after 10 days in S1. (C) Relative maximum respiration of Caco-2 cells exposed to repeated nanoPS in S1 over exposure time. (D) Relative OCR from maximum respiration of Caco-2 cells exposed to different concentrations of nanoPS after 10 days in S1. (E) Relative spare respiratory capacity of Caco-2 cells exposed to repeated nanoPS in S1 over exposure time. (F) Relative OCR from the spare respiratory capacity of Caco-2 cells exposed to different concentrations of nanoPS after 10 days in S1. Caco-2 cells in the culture medium were used as a negative control (100%); $n = 5$. *$p \leq 0.05$, a significant difference compared to the negative control. Yellow squares indicate the statistical significance of at least one nanoPS concentration at specific time points.

S9A, 4-day exposure). Upon repeated dosing, the mitochondrial activity of Caco-2 cells recovered to the level of untreated cells at intermediate time points (6 and 8 days) and reached a high peak at 10 days (Figure S9B), while it decreased to the level of untreated cells after 12 days. For ROS production in S1 (Figure S8B), Caco-2 cells exhibited significant ROS production at high

https://doi.org/10.1021/acs.est.3c10868
Environ. Sci. Technol. 2024, 58, 9967−9979

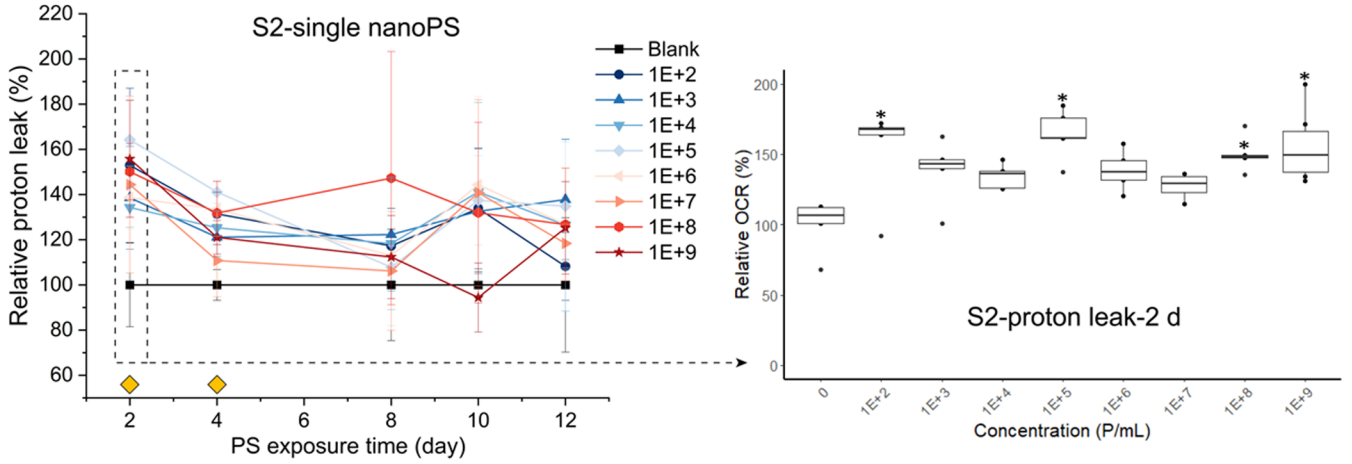

Figure 4. (A) Relative proton leak of Caco-2 cells exposed to a single treatment of nanoPS in S2 over postexposure time. (B) Relative oxygen consumption rate (OCR) from proton leak of Caco-2 cells exposed to different concentrations of nanoPS after 2 days of culture in S2; $n = 5$. $^*p \leq 0.05$, a significant difference compared with untreated cells. Yellow squares indicate the statistical significance of at least one nanoPS concentration at specific time points.

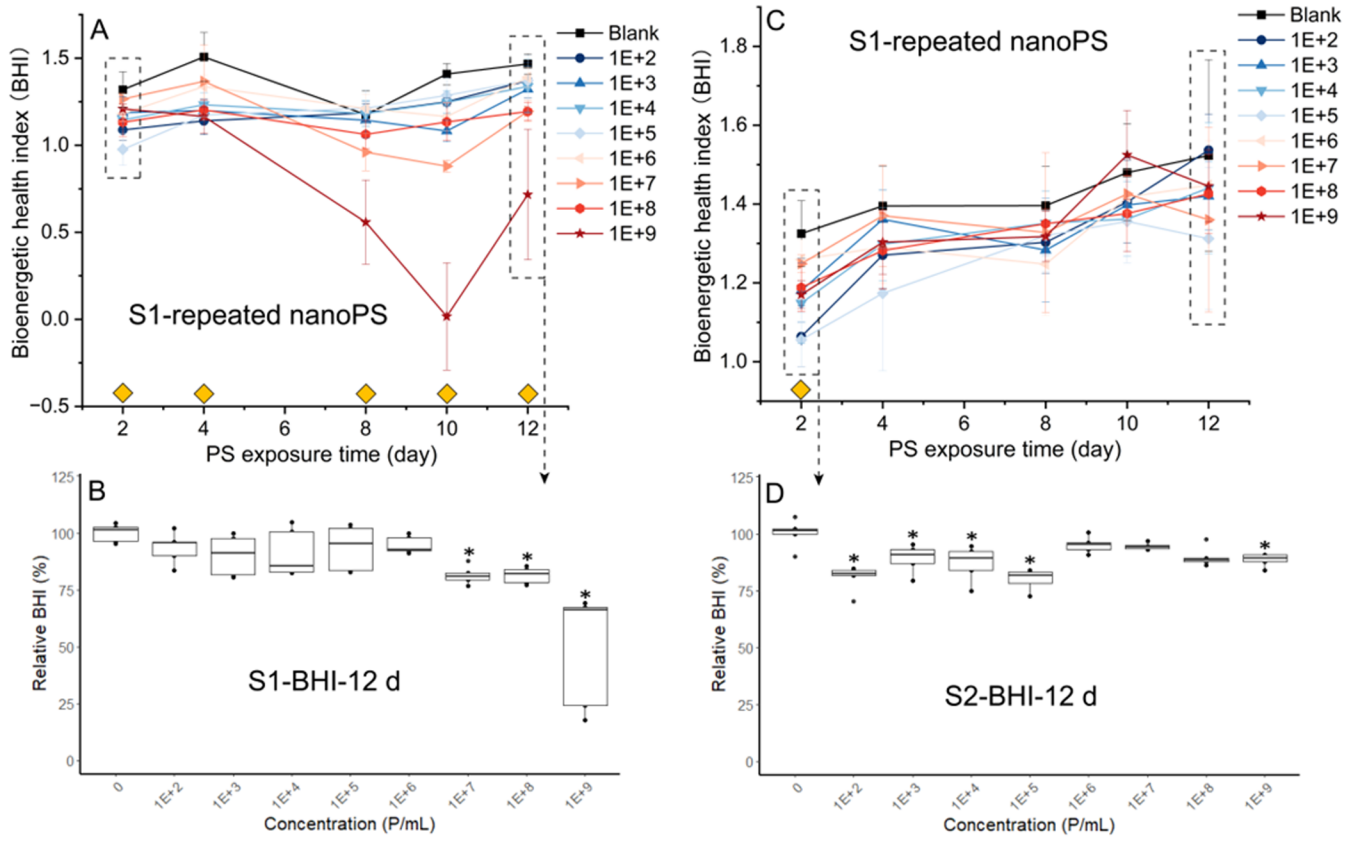

Figure 5. (A) Bioenergetic health index (BHI) of Caco-2 cells repeatedly exposed to nanoPS in scenario 1 (S1) over exposure time (see details of the time point with a dashed rectangle in Figure S15B). (B) Relative BHI of Caco-2 cells exposed to different concentrations of nanoPS after 12 days in S1. (C) BHI of Caco-2 cells exposed to a single treatment of nanoPS in scenario 2 (S2) over postexposure time (see details of the time point with a dashed rectangle in Figure S15D). (D) Relative BHI of Caco-2 cells exposed to different concentrations of nanoPS after 2 days of culture in S2. Caco-2 cells in the culture medium were used as a negative control (100%); $n = 5$. $^*p \leq 0.05$, a significant difference compared to the negative control. Yellow squares indicate the statistical significance of at least one nanoPS concentration at specific time points.

PS doses (from 10^6 P/mL, Figure S9C) after 4 days of exposure. After that, ROS production tended to decline to a level similar to that of untreated cells. However, a single dose of NPs (scenario 2, S2) resulted in both higher mitochondrial activity and ROS production after 4 days (Figures S8C–D and S10A,B). With increasing culture time and continuous medium renewal, mitochondrial activity at all tested PS concentrations gradually decreased to the basal level of untreated cells after 12 days. ROS production gradually decreased until day 10, and then significantly increased after 12 days of culture (Figure S10C).

3.2. Affected Energy Metabolic Pathways. *3.2.1. Real-Time Mitochondrial Respiration.* Six key parameters of the

https://doi.org/10.1021/acs.est.3c10868
Environ. Sci. Technol. 2024, 58, 9967−9979

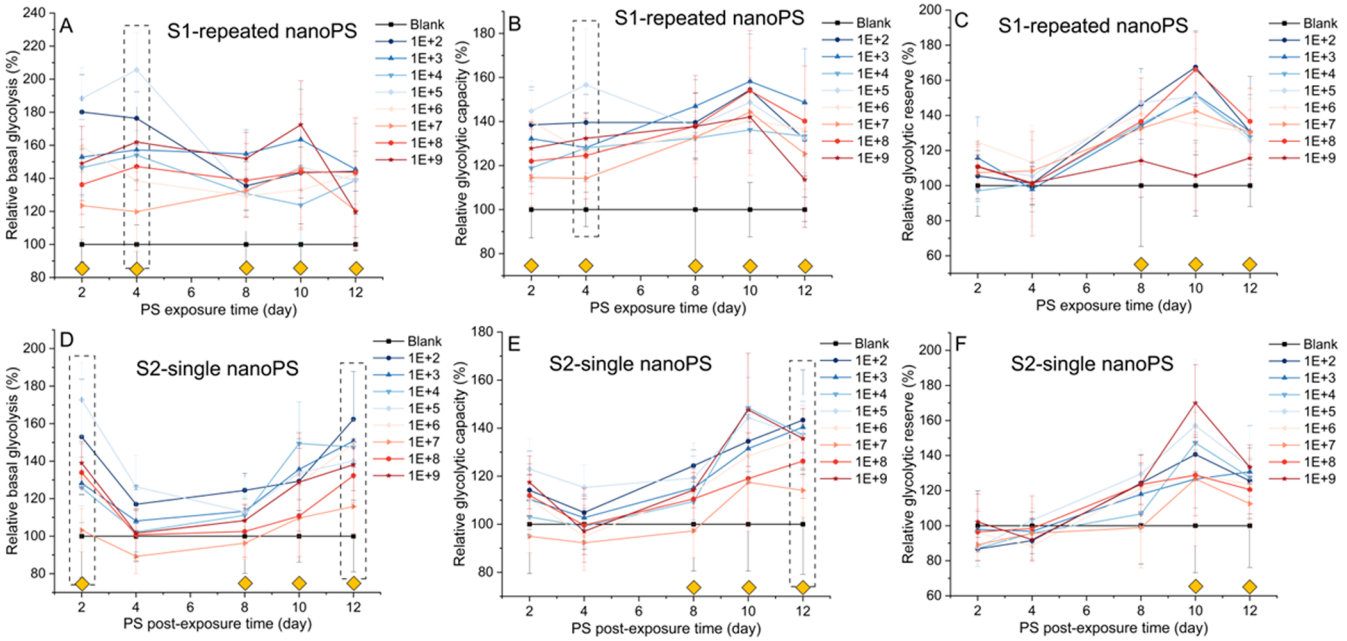

Figure 6. Glycolytic functions of Caco-2 cells exposed to repeated nanoPS in scenario 1 (S1) over exposure time, including (A) basal glycolysis, (B) glycolytic capacity, and (C) glycolytic reserve. Glycolytic functions of Caco-2 cells exposed to single nanoPS in scenario 2 (S2) over postexposure time, including (D) basal glycolysis, (E) glycolytic capacity, and (F) glycolytic reserve. Caco-2 cells in a culture medium were used as a negative control (100%); $n = 5$. Yellow squares indicate the statistical significance of at least one nanoPS concentration at specific time points. The details of the time points with dashed rectangles are shown in Figures S16–S19.

electron transfer chain (ETC) during mitochondrial respiration were measured by subsequent injection of inhibitors (oligomycin, FCCP, and a mixture of rotenone and antimycin A) (Figure 2A). In scenario 1, all mitochondrial parameters were significantly affected by repeated nanoPS exposure. First, nanoPS treatment resulted in a significant increase in proton leakage compared to untreated cells during the whole exposure period (Figures 2B and S11B). In contrast, basal respiration was similar to that of the untreated cells until day 8 (Figure 2C), then it decreased to 58% at the highest nanoPS concentration (10^9 P/mL) after a 10-day repeated exposure and onward (Figure 2D–E). The highest nanoPS concentration resulted in the steepest time response (Figure 2F). Based on the responses over time, ATP-linked respiration and maximum respiration showed the largest dose–response trend after 10 days of exposure (Figures 3A–D and S12–S13). The decrease of spare respiratory capacity was similar to maximum respiration, except that the lowest value (5%) was observed at the highest nanoPS after 10 days of exposure (Figures 3E,F and S14A). Nonmitochondrial respiration followed a similar time- and dose-dependent response to spare respiratory capacity (Figure S15). One difference was that all tested concentrations caused a significant decrease after 10-day repeated exposure (Figure S15C). In contrast, in scenario 2, the initial PS treatment did not cause significant effects on basal respiration, ATP-linked respiration, maximum respiration, spare respiratory capacity, and nonmitochondrial respiration (Figures S16–S20) during long-term culture. Only proton leak significantly increased after 2 days (Figure 4A,B), which then slowly decreased to the same level as untreated cells after 8 day culture and onward.

3.2.2. Bioenergetic Health Index. The bioenergetic health index (BHI) provides an integrated perspective of all mitochondrial parameters described individually in the previous sections as a proxy for mitochondrial health. In scenario 1, the BHI values were always lower than the negative control during the whole repeated exposure (Figures 5A,B and S21A,B). In particular, BHI values significantly declined from day 4 onward for the two highest concentrations (Figure 5A). In scenario 2 (Figures 5C–D and S21C–D), the BHI values of Caco-2 cells were significantly lower than those of the untreated cells after 2 days (Figure 5D); however, with increasing culture time, the BHI curves of Caco-2 cells treated with nanoPS were closer to the curve of untreated cells (black line).

3.2.3. Real-Time Glycolytic Functions. In scenario 1 with repeated nanoPS exposure every 2 days, basal glycolysis was significantly increased after 4 days but without a clear time–response pattern (Figures 6A and S22). Glycolytic capacity (Figures 6B and S23) showed a steady level with significant stimulation at the beginning of repeated exposure, while a time-dependent increased pattern was observed from 4 to 10 days. Caco-2 cells showed a small decrease in glycolytic capacity at 12 days compared to the 10-day exposure. The glycolytic reserve did not show a significant response at early timeslots and then gradually increased until day 12 (Figures 6C and S26A). In scenario 2, basal glycolysis showed a time-dependent response with significantly higher effects after exposure for 2 and 8 days (Figures 6D and S24). Glycolytic capacity showed an increased response over time and was significantly elevated on day 12 (Figures 6E and S25B). The glycolytic reserve showed a similar response to that observed in scenario 1 (Figure 6C,F).

3.2.4. ATP Production Rates. In scenario 1, the ATP production rate produced from mitochondrial respiration (mitoATP) exhibited the same response as ATP-linked respiration with a large decrease at the highest nanoPS after 10 days (Figure S27A,B). Similarly, the glycolytic ATP production rate (glycoATP) (Figure S28A,B) was similar to that of basal glycolysis, but the increased percentages were higher than those in the curves of basal glycolysis. In scenario 2, mitoATP showed the same response as ATP-linked respiration without significant effects over the whole culture period (Figure

https://doi.org/10.1021/acs.est.3c10868
Environ. Sci. Technol. 2024, 58, 9967–9979

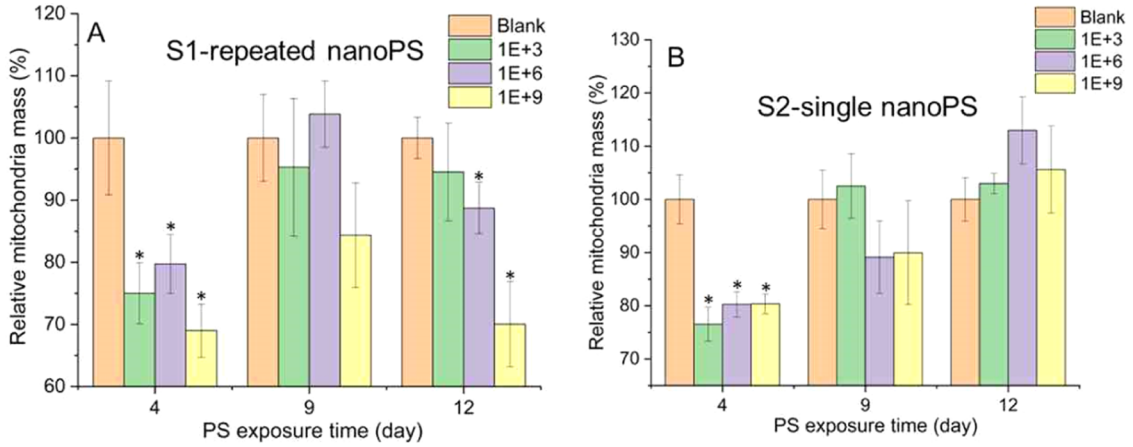

Figure 7. Relative mitochondrial mass of Caco-2 cells exposed to different concentrations (0, 10^3, 10^6, and 10^9 P/mL) of nanoPS in scenario 1 (A) and scenario 2 (B) after 4, 9, and 12 days. Caco-2 cells in the culture medium were used as a negative control (100%); $n = 3$. *$p \leq 0.05$, a significant difference compared to the negative control.

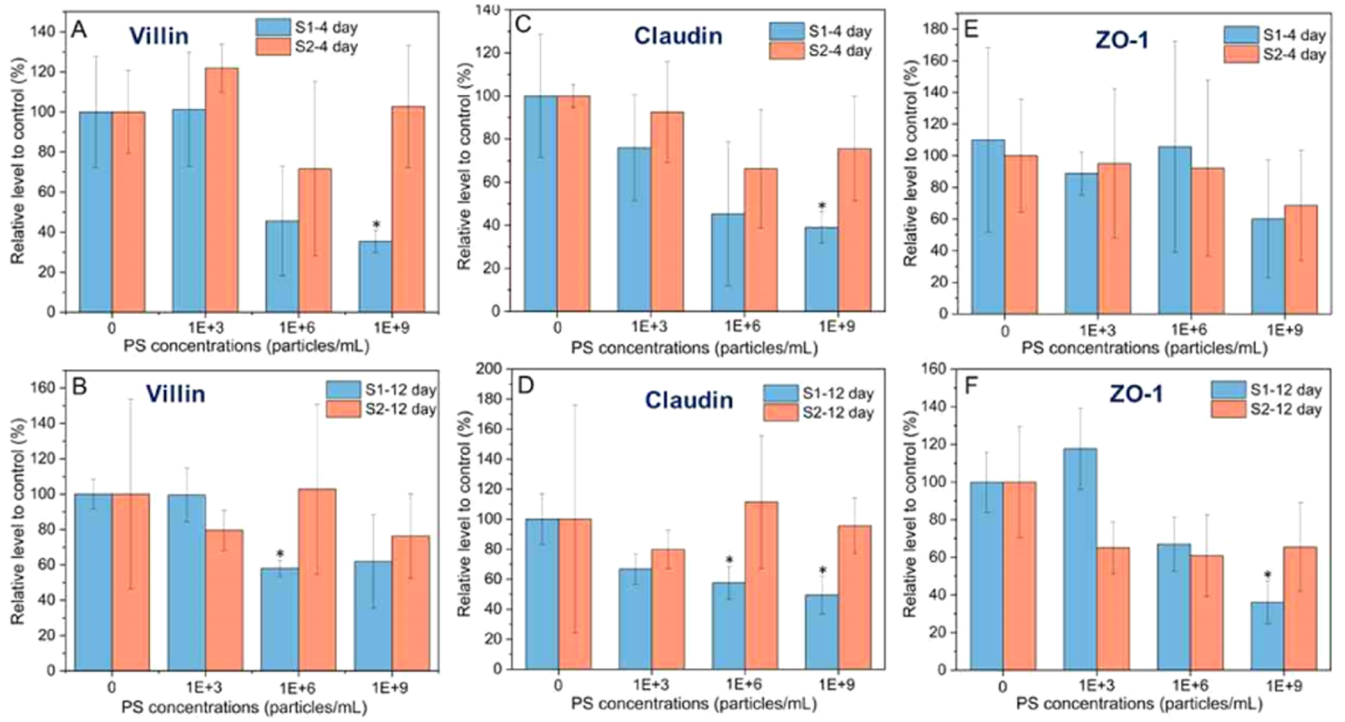

Figure 8. Relative villin expression in Caco-2 cells exposed to different concentrations (0, 10^3, 10^6, and 10^9 P/mL) of nanoPS in scenario 1 (S1) and scenario 2 (S2) after 4 days (A) and 12 days (B). Relative claudin expression in Caco-2 cells exposed to different concentrations (0, 10^3, 10^6, and 10^9 P/mL) of nanoPS in S1 and S2 after 4 days (C) and 12 days (D). Relative ZO-1 expression in Caco-2 cells exposed to different concentrations (0, 10^3, 10^6, and 10^9 P/mL) of nanoPS in S1 and S2 after 4 days (E) and 12 days (F). Caco-2 cells in the culture medium were used as a negative control (100%); $n = 3$. *$p \leq 0.05$, a significant difference compared to the negative control.

S27C−D). The response−time curves of glycoATP (Figure S28C−D) were similar to those of basal glycolysis, showing significant stimulation in the early culture timeslot (2 days). Then, glycoATP slowly reduced until day 8, while it increased to the initial level with a clearly visible increase after day 12.

3.3. Effects on Mitochondrial Mass. In scenario 1, repeated nanoPS exposure seems to induce a cyclic effect with a significant decrease in mitochondrial mass after 4 days at all concentrations and a significant reduction at the end of the repeated exposure for the high nanoPS (12 days, Figure 7A). In scenario 2, the mitochondrial mass was significantly lower after 4 days compared to that in untreated cells (Figure 7B). Later, the mitochondrial mass recovered to a level similar to that of the untreated control without any significant effects from day 9 onward.

3.4. Effects on the Cell Differentiation Process. In scenario 1 with repeated PS treatment, villin and claudin expression was significantly suppressed by the highest PS (10^9 P/mL) after 4 days (Figure 8A,C). At the end of the exposure time (12 days), all proteins showed decreased expression at high concentrations, which was protein-specific (Figure 8B,D,F). However, none of the investigated proteins showed any significant response after 4 and 12 days of single exposure under scenario 2 (Figure 8).

https://doi.org/10.1021/acs.est.3c10868
Environ. Sci. Technol. 2024, 58, 9967−9979

Additionally, Caco-2 cells exposed to different concentrations of nanoPS in both scenarios were visualized using light microscopy at the end of the exposure period (12 days). In scenario 1 with repeated nanoPS exposure, Caco-2 cells treated with high concentrations (10^6 and 10^9 P/mL) were more irregular and fuzzy (Figure S29). Nevertheless, in scenario 2 with single dosing, the cell membranes of Caco-2 cells were clearly observed in all samples (Figure S30).

4. DISCUSSION

In this study, we illustrate that (i) initial subtle impacts on mitochondria by low concentrations could accumulate and finally lead to significant damage to mitochondrial functions and cell differentiation process with repeated dosing under long-term exposure, (ii) the mitochondrial perturbance by single dosing of nanoPS at low concentrations does not persist over long-term postexposure, likely due to self-recovery capacity, and (iii) the secondary effects, even of single dosing, occur at a late postexposure time after the initial stressor has been removed, likely due to dynamic transport of nanoPS and cellular functions.

First, Caco-2 cells in scenario 1 exhibited a dynamic cellular response and underwent several phases. These dynamic decreases and increases in mitochondrial activity and ROS production, respectively, suggest that cells continue to struggle to survive long-term stress from repeated nanoPS during hormesis, apoptosis, proliferation, and differentiation. In contrast, Caco-2 cells suffered from oxidative stress at the beginning of the postexposure period (4 days after initial nanoPS addition) in scenario 2. This level of ROS production could trigger signaling pathways that promote cell survival in response to mild oxidative stress,[32] leading to significantly increased mitochondrial activity that was observed after 4 days in the MTT assay. With continuously renewing the culture medium during the following long-term culture, none of the tested nanoPS concentrations induced effects on mitochondrial activity at the end of the culture (after 12 days). This result may be attributed to two reasons: (1) Caco-2 cells could undergo apoptosis, proliferation, and differentiation during long-term growth, and thus, the previously affected cells could be replaced by new healthy cells or differentiate into differentiated cells;[33,34] (2) it is widely reported that nanoplastics could be internalized in the cytoplasma, nuclei, and organelles as well as adhere to the surface of cells.[35] Meanwhile, the internalized nanoplastics could be excreted from cells via energy-free penetration and energy-dependent lysosomal exocytosis.[36] Thus, nanoPS might be internalized in Caco-2 cells during the early period and subsequently excreted from cells during consistent culture medium renewal. Interestingly, ROS production was significantly elevated again at the end of the culture period, and the potential mechanisms of recovery from oxidative stress are elucidated below.

At the metabolic level, in scenario 1, only subtle effects were observed after 2 days of exposure, as evidenced by a significant increase in proton leak. This differs from that reported in acute studies. For instance, with exposure to high concentrations of nanoPS (50 nm) for 24 h, it was found that A549 cells showed increased spare respiratory capacity and proton leak at 5.82×10^{11} P/mL, while decreased spare respiratory capacity and ATP-linked respiration at 2.33×10^{12} P/mL.[20] A study reported that exposure to nanoPS (80 nm, 8.75×10^{11} P/mL) for 48 h caused decreased basal respiration, maximum respiration, ATP-linked respiration, and proton leak in human hepatic L02 cells.[19] From the aspect of short-term exposure (within 48 h), these previously reported effects are much more severe than what was found in our study, which primarily covers the lag phase of the dose–response curve. One primary reason for this difference is that the concentrations used in the literature are 2 to 10 orders of magnitude higher than the environmentally relevant concentrations (10^2–10^9 P/mL concluded from Table S1) used in this study, even if other factors vary.

Remarkably, with consistent, repeated nanoPS exposure, mitochondrial function was significantly inhibited from day 8 onward, as reflected in all mitochondrial parameters (basal respiration, ATP-linked respiration, maximum respiration, spare respiratory capacity, nonmitochondrial respiration, and proton leak). In detail, the decreased basal respiration, representing the baseline mitochondrial oxygen consumption under no stressors, indicated that mitochondrial respiration was inhibited by consistent nanoPS exposure. A reduction in ATP-linked respiration, which refers to the portion of oxygen consumption directly linked to ATP production through oxidative phosphorylation (OXPHOS), suggests that nanoPS disrupts the electron transport chain (ETC) or hinders ATP synthesis. Also, the mitochondrial stress or damage caused by repeated nanoPS exposure may limit the cell's ability to meet increased energy demands or make cells less resilient to energy fluctuations, which is a possible reason for decreased maximum respiration and spare respiratory capacity. Nonmitochondrial respiration is the oxygen consumption that occurs outside the mitochondria and is often linked to enzymes involved in inflammatory processes, such as cyclooxygenases, lipoxygenases, and NADPH oxidases.[37,38] Decreased values may suggest that nonmitochondrial oxygen-consuming processes were compromised by repeated nanoPS exposure as well. In addition, the increased proton leak over the whole exposure indicates that more protons are flowing back into the mitochondrial matrix, bypassing ATP synthase (complex V). This finding could be attributed to several factors, such as increased uncoupling protein (UCP) activity or damage to membrane permeability or the electron transport chain (ETC) caused by nanoPS incorporation.[28] Thus, in scenario 1, once repeated exposure lasts for a long enough time, nanoPS would lead to notable mitochondrial stress, mitochondrial dysfunction, and impairment of mitochondrial membrane permeability and ETC. The change of bioenergetic health index (BHI),[28] an indicator of mitochondrial health, quantitatively depicted the dynamic transition, where the BHI values of nanoPS-treated Caco-2 cells were far below those of untreated cells, indicative of compromised mitochondrial health.

Overall, the initial slight impacts on mitochondrial respiration (ETC and OXPHOS) by low concentrations would accumulate upon repeated nanoPS exposure and finally lead to significantly impaired mitochondrial functions that are much more serious than acute toxicity at high concentrations. These findings complement the previously documented short-term effects and exhibit possible heightened mitochondrial stress and impairment resulting from long-term exposure, which are implicated in the potential pathogenesis of various human metabolic disorders such as diabetes and obesity, as well as conditions including cancer, cardiovascular disease, and neurodegeneration.[39] Until now, few studies have explored the long-term effects of nanoPS on cells with repeated exposure.[40−42] Nevertheless, prior investigations predominantly conducted measurements at the end of the exposure period, whereas our study, characterized by the continuous monitoring of dynamic responses throughout the entire exposure duration, facilitates a comprehensive understanding of time-dependent effects. On the other hand,

https://doi.org/10.1021/acs.est.3c10868
Environ. Sci. Technol. 2024, 58, 9967−9979

as indicated by a recent report that there are 16325 compounds with various functions in plastics,[43] there are indeed likely to be chemicals existing together with PS nanoplastics in the stock solution used in our study. This may have potential effects on cells during exposure. Thus, we used GC-MS to analyze four common plasticizers and leachates in the stock solutions (see Supporting File 3). All of them were detected but at concentrations below the LOQ (see details in Table S3). The highest concentration (10^9 particles/mL) used in this study was diluted 10,000 times from the stock solution. As such, the highest possible components that existed during cell exposure were 100 times lower than the values in Table S3. Thus, traces of these compounds cannot be excluded and may affect the cells. We also performed an untargeted analysis and did not identify any additional peaks (see details in Figures S4 and S5 of the SI). Nevertheless, these chemicals can never be fully excluded, also not in real-life scenarios. For instance, surfactants frequently coexist with plastic products throughout the manufacturing process, subsequently entering our environmental milieu.[44] The generation of micro/nanoplastics invariably entails the release of additives in a complex environment.[45] Moreover, the weathering process of micro/nanoplastics results in the discharge of leachates.[46] To some extent, looking into the relevant plastic effects always means looking into the effects of both plastics and coexisting chemicals.

In contrast, glycolytic functions in scenario 1 were significantly elevated over the whole prolonged exposure period. There are some possible explanations for these results: (1) due to impaired mitochondrial functions demonstrated before, to compensate for any mitochondrial dysfunction, Caco-2 cells may rely more on glycolysis to meet their energy needs. This compensation mechanism was indicated in a previous study where glycolysis was increased, while mitochondrial respiration decreased after long-term nanoPS exposure;[40] (2) Caco-2 cells could respond to stress from continuous nanoPS exposure by increasing glycolysis to rapidly generate ATP. This can provide energy for repair mechanisms, including DNA repair, and for coping with oxidative stress; and (3) over time, Caco-2 cells may adapt to nanoPS exposure by modifying their metabolic pathways. Increased glycolysis could be a long-term adaptation to the presence of nanoPS, allowing cells to maintain essential functions despite the stressors.

For the mitochondrial respiration in scenario 2 with single nanoPS dosing, the significant effects on proton leak after 2 days abated, and mitochondria recovered to a healthy state with the continuous renewal of the culture medium during the later postexposure period. These results align with the dynamic change of BHI values, wherein the BHI values of nanoPS-treated Caco-2 cells gradually approached the level of untreated cells from below with increasing recovery time. This further implies a restoration of impaired mitochondrial function to a healthy state during the postexposure period. It has been reported that nanoPS can interact with and be internalized in mitochondria as well as induce mitophagy upon short exposure (24 h).[47] As such, mitochondria may excrete or release internalized nanoPS due to mitochondrial dynamics, including mitophagy, fusion, and fission occurring in long-term culture with continuous culture medium renewal. To the best of our knowledge, this is the first study on the duration of effects on mitochondria after single dosing of nanoPS addition at the initial stage, which suggests that mitochondria have the ability to regulate mitochondrial state and recover from mitochondrial dysfunction due to mitochondrial homeostasis if cells are exposed to nanoPS at environmentally relevant concentrations (based on our current knowledge) once and then renewed with the culture medium. Despite no related studies as a comparison or reference, the dynamic transport of nanoPS in mitochondria over long-term culture could be monitored to support our results in future research. Additionally, we may conclude that the increased ROS levels at the end of scenario 2 are most probably a secondary effect, and hence, not immediately caused by mitochondrial defects.

For the glycolytic functions (glycolysis occurring in the cytoplasm) in scenario 2, a significant stimulation of basal glycolysis at the beginning of the exposure time may lead to a buildup of reducing equivalents (NADH) and an altered redox balance in the cell. This imbalance could increase the likelihood of electron leakage from the ETC and the subsequent generation of ROS, thereby contributing to oxidative stress.[48,49] Thus, higher basal glycolysis may be a reason for the increased ROS production observed at early time points. As the culture time increased and the culture medium renewed, basal glycolysis recovered to the level of untreated cells over the intermediate stage of culture (from 4 to 8 days). Surprisingly, from day 8 day onward, all glycolytic parameters (basal glycolysis, glycolytic capacity, and reserve) were stimulated, in parallel with the increased ROS production observed before, pointing to a secondary or delayed effect occurring from the middle culture time. It is well known that Caco-2 cells spontaneously start to differentiate once confluency is reached, which is typical between 4 and 8 days of culture after confluency.[50] This process is accompanied by profound morphological changes, such as brush-border microvilli formation and tight junction expression. As such, this different morphology may contribute to particle dynamics within cells. For instance, it has been reported that nanoPS can be easily released from CCD-18Co cells[40] but tight junctions of hiPSC colonies can inhibit nanoPS excretion.[51] Similarly, tight junctions of differentiated Caco-2 cells may hinder nanoPS release from cells at a later period of culture. Thus, excreted nanoPS from mitochondria would accumulate in the cytoplasm, leading to oxidative stress on glycolysis and the second increased glycolytic functions. The secondary effect on glycolysis at the late postexposure time in scenario 2 augmented our existing understanding, extending beyond the acute effects observed in short-term exposure.

Mitochondrial mass is a key parameter for monitoring cell proliferation and differentiation, as it reflects the cellular metabolic adaptations and energy demands associated with these processes.[52,53] It is linked to mitochondrial number, size, density, and content. In scenario 1, the lower mitochondrial mass of nanoPS-treated Caco-2 cells at day 4 further aligns with the slight damage to mitochondrial respiration observed at the early culture time. As repeated exposure lasted, Caco-2 cells tried to overcome the stress from repeated nanoPS exposure, and thus, the recovered mitochondrial mass was observed after 9 days. However, once the accumulation of nanoPS and stress reached a high level (threshold), Caco-2 cells likely gave up the defense and thus mitochondria were impaired significantly, which could explain the reduced mitochondrial mass at the end of the exposure. In addition, the dynamic change of mitochondrial mass corresponds to and could be the reason for the change of mitochondrial activity. A study found that mouse cells showed significant mitochondrial mass loss induced by 21-day sepsis as well.[54] For scenario 2, the early effects on mitochondrial mass were similar to scenario 1, which showed decreased mass owing to mitochondrial dysfunction. As time

https://doi.org/10.1021/acs.est.3c10868
Environ. Sci. Technol. 2024, 58, 9967−9979

increased and the culture medium was renewed, the mitochondrial mass gradually recovered to the level of untreated cells, which further reflected a healthy mitochondrial state in the final period. Similarly, a study demonstrated that decreased mitochondrial mass by cigarette smoke extract (CSE) was recovered when CSE-treated BEAS-2B cells grew in a culture medium for 3 months.[55]

As a typical epithelial cell type, Caco-2 cells display some special morphological features (tight junctions and brush-border microvilli development) that are linked to differentiation during long-term culture. Thus, the protein characteristics of these typical morphologies are villin-a molecular marker of brush-border development,[56,57] claudin-tight junction protein,[58] and zonula occludens-1 (ZO-1)-junctional adaptor protein.[59] According to our previous experience,[17,26,60] Caco-2 cells without any treatment undergo a differentiation process upon long-term culture, which was regarded as a reference or blank control to check the differentiation progress of cells treated with nanoPS in two dosing patterns. With this in mind, in scenario 1, repeated nanoPS exposure inhibited the expression of the three markers at intermediate and high concentrations (10^6 and 10^9 P/mL) at the end of exposure time, which indicates that the formation of the brush border and tight junctions was affected by continuous nanoPS exposure. Thus, it is deduced that the differentiation progress of Caco-2 cells was hindered by repeated exposure, which corresponds well with the microscopy images that nanoPS-treated cells (10^6 and 10^9 P/mL) showed abnormal morphology compared to untreated cells. The influenced differentiation process could be due to impaired mitochondria that could not provide the required energy for cell differentiation.[61] However, the expression of the three markers was not affected by all tested nanoPS over the whole culture time in a single exposure, which in parallel with the microscopic analysis suggests that Caco-2 cells with single nanoPS exposure undergo a differentiation process smoothly, which could be a support for the secondary effects on glycolysis at the end of the postexposure period.

This study shows, for the first time, innovative findings that repeated exposure to nanoPS at low concentrations causes significant damage to mitochondria and suppresses cell differentiation under prolonged exposure. Consistent mitochondrial stress and impairment are determinants in the emergence of many chronic diseases. Single dosing of nanoPS evoked transient effects on mitochondria, while the self-recovery capacity of Caco-2 cells eliminated these effects, and the cell differentiation process was not affected during long-term homeostasis, although some stress effects appeared during later differentiation. This study helps us further understand the toxicity of nanoplastics in real life and provides potential suggestions for the frequency and habit of daily use of plastic products. Meanwhile, it has some limitations and perspectives: (1) only in vitro cell models were implemented in this study, and future studies can be expanded to in vivo models to gain a comprehensive assessment of nanoplastics risk; (2) the visualization of internalization and excretion of nanoplastics should be conducted to further understand dynamic transport during two long-term scenarios in the future; (3) molecular analysis such as related expression of cytokines, proteins, and genes should be performed in two scenarios in the future; and (4) spherical PS plastic particles used in this study could be expanded to include multidimensional characteristics (multiple polymer types like polypropylene (PP), polyethylene (PE), and poly(ethylene terephthalate) (PET), irregular shapes or morphology, and surface functional groups) to make samples closer to environmental conditions.

5. IMPLICATIONS

In this study, Caco-2 cells were exposed to nanoPS at an environmentally relevant concentration range (10^2–10^9 particles/mL) under two different scenarios, where nanoPS was repeatedly added to cells every 2 days for a 12-day repeated exposure while nanoPS was only added to cells once and then the treated cells were cultured for 12 days in another case. In the former case, mitochondrial respiration and cell differentiation were largely inhibited at the end of long-term exposure. At the same time, continuous nanoPS exposure reduced mitochondrial mass in the final period. In the latter case, nanoPS induced transient damage in the mitochondria and increased ROS production at the beginning of exposure, but these effects disappeared at later culture times. Instead, glycolytic functions were stimulated at the end of the culture period, accompanied by elevated ROS production, while the cell differentiation process and mitochondrial mass were not affected over the whole culture period. This work is the first to study the toxicity of NPs in simulated realistic long-term exposure scenarios, which is of great significance in assessing the health hazards posed by NPs during our lifespan.

■ ASSOCIATED CONTENT

Supporting Information

The Supporting Information is available free of charge at https://pubs.acs.org/doi/10.1021/acs.est.3c10868.

Detailed information on the summary of studies detecting nanoplastics in the environment (Table S1); characterization of nanoplastics, including scanning electron microscopy (SEM) (Figure S1); dynamic light scattering (DLS) (Table S2 and Figures S2–S3); additives and leachates (Table S3 and Figures S4–S5); experimental design (Figure S6); gating strategy to measure mitochondrial mass (Figure S7); detailed results of MTT, and ROS assays (Figures S8–S10); detailed results of the seahorse analyzer (Figure S11–S28), and microscopic images of cells during exposure scenarios (Figures S29–S30) (PDF)

■ AUTHOR INFORMATION

Corresponding Author

Andreja Rajkovic − *Department of Food Technology, Safety and Health, Faculty of Bioscience Engineering, Ghent University, 9000 Ghent, Belgium*; Email: Andreja.Rajkovic@UGent.be

Authors

Miao Peng − *Laboratory of Environmental Toxicology and Aquatic Ecology, Faculty of Bioscience Engineering, Ghent University, 9000 Ghent, Belgium; Blue Growth Research Lab, Ghent University, 8400 Oostende, Belgium;* orcid.org/0000-0002-8005-1988

Charlotte Grootaert − *Department of Food Technology, Safety and Health, Faculty of Bioscience Engineering, Ghent University, 9000 Ghent, Belgium*

Maaike Vercauteren − *Laboratory of Environmental Toxicology and Aquatic Ecology, Faculty of Bioscience Engineering, Ghent University, 9000 Ghent, Belgium; Blue*

https://doi.org/10.1021/acs.est.3c10868
Environ. Sci. Technol. 2024, 58, 9967−9979

Growth Research Lab, Ghent University, 8400 Oostende, Belgium; orcid.org/0000-0002-7618-143X

Nico Boon − *Center for Microbial Technology and Ecology (CMET), Faculty of Bioscience Engineering, Ghent University, 9000 Ghent, Belgium;* orcid.org/0000-0002-7734-3103

Colin Janssen − *Laboratory of Environmental Toxicology and Aquatic Ecology, Faculty of Bioscience Engineering, Ghent University, 9000 Ghent, Belgium; Blue Growth Research Lab, Ghent University, 8400 Oostende, Belgium*

Jana Asselman − *Laboratory of Environmental Toxicology and Aquatic Ecology, Faculty of Bioscience Engineering, Ghent University, 9000 Ghent, Belgium; Blue Growth Research Lab, Ghent University, 8400 Oostende, Belgium;* orcid.org/0000-0003-0185-6516

Complete contact information is available at: https://pubs.acs.org/10.1021/acs.est.3c10868

Author Contributions

⊥A.R. and J.A. contributed equally to this work.

Notes

The authors declare no competing financial interest.

■ ACKNOWLEDGMENTS

M.P. is currently pursuing a doctoral degree with financial support from the China Scholarship Council (CSC) under File No. 201906150135 and the UGent Special Research Fund (BOFCHN2019000801). M.V. is a recipient of funding through the BOF Research Grant with the code BOF21/PDO/081. We extend our appreciation to Ghent University's Special Research Fund for their generous support in procuring the Seahorse equipment under grant BOF.BAS.2020.0035.01 and the flow cytometer under grant BOF.BAS.2022.0014.01. This research received partial funding from the ImpTox project, which was sponsored by the European Union's Horizon 2020 research and innovation program under grant No. 965173.

■ REFERENCES

(1) Zangmeister, C. D.; Radney, J. G.; Benkstein, K. D.; Kalanyan, B. Common Single-Use Consumer Plastic Products Release Trillions of Sub-100 nm Nanoparticles per Liter into Water during Normal Use. *Environ. Sci. Technol.* **2022**, *56* (9), 5448−5455.

(2) Li, D.; Shi, Y.; Yang, L.; Xiao, L.; Kehoe, D. K.; Gun'ko, Y. K.; Boland, J. J.; Wang, J. J. Microplastic release from the degradation of polypropylene feeding bottles during infant formula preparation. *Nat. Food* **2020**, *1* (11), 746−754.

(3) Hussain, K. A.; Romanova, S.; Okur, I.; Zhang, D.; Kuebler, J.; Huang, X.; Wang, B.; Fernandez-Ballester, L.; Lu, Y.; Schubert, M.; Li, Y. Assessing the Release of Microplastics and Nanoplastics from Plastic Containers and Reusable Food Pouches: Implications for Human Health. *Environ. Sci. Technol.* **2023**, *57* (26), 9782−9792.

(4) Hernandez, L. M.; Xu, E. G.; Larsson, H. C. E.; Tahara, R.; Maisuria, V. B.; Tufenkji, N. Plastic Teabags Release Billions of Microparticles and Nanoparticles into Tea. *Environ. Sci. Technol.* **2019**, *53* (21), 12300−12310.

(5) Zhang, J.; Peng, M.; Lian, E.; Xia, L.; Asimakopoulos, A. G.; Luo, S.; Wang, L. Identification of Poly(ethylene terephthalate) Nanoplastics in Commercially Bottled Drinking Water Using Surface-Enhanced Raman Spectroscopy. *Environ. Sci. Technol.* **2023**, *57* (22), 8365−8372.

(6) Berglund, E.; Fogelberg, V.; Nilsson, P. A.; Hollander, J. Microplastics in a freshwater mussel (Anodonta anatina) in Northern Europe. *Sci. Total Environ.* **2019**, *697*, No. 134192.

(7) Tien, C.-J.; Wang, Z.-X.; Chen, C. S. Microplastics in water, sediment and fish from the Fengshan River system: Relationship to aquatic factors and accumulation of polycyclic aromatic hydrocarbons by fish. *Environ. Pollut.* **2020**, *265*, No. 114962.

(8) Gautam, R.; Jo, J.; Acharya, M.; Maharjan, A.; Lee, D.; C, P. B. K.; Kim, C.; Kim, K.; Kim, H.; Heo, Y. Evaluation of potential toxicity of polyethylene microplastics on human derived cell lines. *Sci. Total Environ.* **2022**, *838*, No. 156089.

(9) Wang, H.; Shi, X.; Gao, Y.; Zhang, X.; Zhao, H.; Wang, L.; Zhang, X.; Chen, R. Polystyrene nanoplastics induce profound metabolic shift in human cells as revealed by integrated proteomic and metabolomic analysis. *Environ. Int.* **2022**, *166*, No. 107349.

(10) Cortés, C.; Domenech, J.; Salazar, M.; Pastor, S.; Marcos, R.; Hernández, A. Nanoplastics as a potential environmental health factor: effects of polystyrene nanoparticles on human intestinal epithelial Caco-2 cells. *Environ. Sci.: Nano* **2020**, *7* (1), 272−285.

(11) Dong, C.-D.; Chen, C.-W.; Chen, Y.-C.; Chen, H.-H.; Lee, J.-S.; Lin, C.-H. Polystyrene microplastic particles: In vitro pulmonary toxicity assessment. *J. Hazard. Mater.* **2020**, *385*, No. 121575.

(12) O'Neill, S. M.; Lawler, J. Knowledge gaps on micro and nanoplastics and human health: A critical review. *Case Stud. Chem. Environ. Eng.* **2021**, *3*, No. 100091.

(13) Molina, E.; Benedé, S. Is There Evidence of Health Risks From Exposure to Micro- and Nanoplastics in Foods? *Front. Nutr.* **2022**, *9*, No. 100091.

(14) Sukkar, S. G.; Bassetti, M. Induction of ketosis as a potential therapeutic option to limit hyperglycemia and prevent cytokine storm in COVID-19. *Nutrition* **2020**, *79*−*80*, No. 110967.

(15) Van den Berghe, G. How does blood glucose control with insulin save lives in intensive care? *J. Clin. Invest.* **2004**, *114* (9), 1187−1195.

(16) von Kleist-Retzow, J.-C.; Hornig-Do, H.-T.; Schauen, M.; Eckertz, S.; Dinh, T. A. D.; Stassen, F.; Lottmann, N.; Bust, M.; Galunska, B.; Wielckens, K.; Hein, W.; Beuth, J.; Braun, J.-M.; Fischer, J. H.; Ganitkevich, V. Y.; Maniura-Weber, K.; Wiesner, R. J. Impaired mitochondrial Ca2+ homeostasis in respiratory chain-deficient cells but efficient compensation of energetic disadvantage by enhanced anaerobic glycolysis due to low ATP steady state levels. *Exp. Cell Res.* **2007**, *313* (14), 3076−3089.

(17) Peng, M.; Vercauteren, M.; Grootaert, C.; Rajkovic, A.; Boon, N.; Janssen, C.; Asselman, J. Cellular and bioenergetic effects of polystyrene microplastic in function of cell type, differentiation status and post-exposure time. *Environ. Pollut.* **2023**, *337*, No. 122550.

(18) Peng, M.; Vercauteren, M.; Grootaert, C.; Catarino, A. I.; Everaert, G.; Rajkovic, A.; Janssen, C.; Asselman, J. Bioenergetic effects of pristine and ultraviolet-weathered polydisperse polyethylene terephthalate and polystyrene nanoplastics on human intestinal Caco-2 cells. *Sci. Total Environ.* **2024**, *908*, No. 168267.

(19) Lin, S.; Zhang, H.; Wang, C.; Su, X.-L.; Song, Y.; Wu, P.; Yang, Z.; Wong, M.-H.; Cai, Z.; Zheng, C. Metabolomics Reveal Nanoplastic-Induced Mitochondrial Damage in Human Liver and Lung Cells. *Environ. Sci. Technol.* **2022**, *56* (17), 12483−12493.

(20) Halimu, G.; Zhang, Q.; Liu, L.; Zhang, Z.; Wang, X.; Gu, W.; Zhang, B.; Dai, Y.; Zhang, H.; Zhang, C.; Xu, M. Toxic effects of nanoplastics with different sizes and surface charges on epithelial-to-mesenchymal transition in A549 cells and the potential toxicological mechanism. *J. Hazard. Mater.* **2022**, *430*, No. 128485.

(21) Almeida, L.; Dhillon-LaBrooy, A.; Carriche, G.; Berod, L.; Sparwasser, T. CD4+ T-cell differentiation and function: Unifying glycolysis, fatty acid oxidation, polyamines NAD mitochondria. *J. Allergy Clin. Immunol.* **2021**, *148* (1), 16−32.

(22) Xu, X.; Duan, S.; Yi, F.; Ocampo, A.; Liu, G.-H.; Belmonte, J. C. I. Mitochondrial Regulation in Pluripotent Stem Cells. *Cell Metab.* **2013**, *18* (3), 325−332.

(23) Mitra, K. Mitochondrial fission-fusion as an emerging key regulator of cell proliferation and differentiation. *BioEssays* **2013**, *35* (11), 955−964.

(24) Ren, L.; Chen, X.; Chen, X.; Li, J.; Cheng, B.; Xia, J. Mitochondrial Dynamics: Fission and Fusion in Fate Determination of Mesenchymal Stem Cells. *Front. Cell Dev. Biol.* **2020**, *8*, No. 580070.

(25) Wu, T.; Grootaert, C.; Voorspoels, S.; Jacobs, G.; Pitart, J.; Kamiloglu, S.; Possemiers, S.; Heinonen, M.; Kardum, N.; Glibetic, M.;

Smagghe, G.; Raes, K.; Van Camp, J. Aronia (Aronia melanocarpa) phenolics bioavailability in a combined in vitro digestion/Caco-2 cell model is structure and colon region dependent. *J. Funct. Foods* **2017**, *38*, 128−139.
(26) Geirnaert, A.; Calatayud, M.; Grootaert, C.; Laukens, D.; Devriese, S.; Smagghe, G.; De Vos, M.; Boon, N.; Van de Wiele, T. Butyrate-producing bacteria supplemented in vitro to Crohn's disease patient microbiota increased butyrate production and enhanced intestinal epithelial barrier integrity. *Sci. Rep.* **2017**, *7* (1), No. 11450.
(27) Chacko, B. K.; Zhi, D.; Darley-Usmar, V. M.; Mitchell, T. The Bioenergetic Health Index is a sensitive measure of oxidative stress in human monocytes. *Redox Biol.* **2016**, *8*, 43−50.
(28) Chacko, B. K.; Kramer, P. A.; Ravi, S.; Benavides, G. A.; Mitchell, T.; Dranka, B. P.; Ferrick, D.; Singal, A. K.; Ballinger, S. W.; Bailey, S. M.; Hardy, R. W.; Zhang, J.; Zhi, D.; Darley-Usmar, V. M. The Bioenergetic Health Index: a new concept in mitochondrial translational research. *Clin. Sci.* **2014**, *127* (6), 367−373.
(29) Doherty, E.; Perl, A. Measurement of Mitochondrial Mass by Flow Cytometry during Oxidative Stress. *React. Oxygen Species* **2017**, *4* (10), 275−283.
(30) de Brito Monteiro, L.; Davanzo, G. G.; de Aguiar, C. F.; Moraes-Vieira, P. M. M. Using flow cytometry for mitochondrial assays. *MethodsX* **2020**, *7*, No. 100938.
(31) Ritz, C.; Streibig, J. C. Bioassay Analysis Using R. *J. Stat. Software* **2005**, *12* (5), 1−22.
(32) Moloney, J. N.; Cotter, T. G. ROS signalling in the biology of cancer. *Semin. Cell Dev. Biol.* **2018**, *80*, 50−64.
(33) Tremblay, E.; Auclair, J.; Delvin, E.; Levy, E.; Ménard, D.; Pshezhetsky, A. V.; Rivard, N.; Seidman, E. G.; Sinnett, D.; Vachon, P. H.; Beaulieu, J.-F. Gene expression profiles of normal proliferating and differentiating human intestinal epithelial cells: A comparison with the Caco-2 cell model. *J. Cell. Biochem.* **2006**, *99* (4), 1175−1186.
(34) Van De Walle, J.; Hendrickx, A.; Romier, B.; Larondelle, Y.; Schneider, Y.-J. Inflammatory parameters in Caco-2 cells: Effect of stimuli nature, concentration, combination and cell differentiation. *Toxicol. In Vitro* **2010**, *24* (5), 1441−1449.
(35) Hua, X.; Wang, D. Cellular Uptake, Transport, and Organelle Response After Exposure to Microplastics and Nanoplastics: Current Knowledge and Perspectives for Environmental and Health Risks. *Rev. Environ. Contam. Toxicol.* **2022**, *260* (1), No. 12.
(36) Liu, L.; Xu, K.; Zhang, B.; Ye, Y.; Zhang, Q.; Jiang, W. Cellular internalization and release of polystyrene microplastics and nanoplastics. *Sci. Total Environ.* **2021**, *779*, No. 146523.
(37) Cho, K.-J.; Seo, J.-M.; Kim, J.-H. Bioactive Lipoxygenase Metabolites Stimulation of NADPH Oxidases and Reactive Oxygen Species. *Mol. Cells* **2011**, *32* (1), 1−6.
(38) Pendyala, S.; Natarajan, V. Redox regulation of Nox proteins. *Respir. Physiol. Neurobiol.* **2010**, *174* (3), 265−271.
(39) Chen, Y.; Huang, T.; Yu, Z.; Yu, Q.; Wang, Y.; Hu, Ja.; Shi, J.; Yang, G. The functions and roles of sestrins in regulating human diseases. *Cell. Mol. Biol. Lett.* **2022**, *27* (1), No. 2.
(40) Bonanomi, M.; Salmistraro, N.; Porro, D.; Pinsino, A.; Colangelo, A. M.; Gaglio, D. Polystyrene micro and nano-particles induce metabolic rewiring in normal human colon cells: A risk factor for human health. *Chemosphere* **2022**, *303*, No. 134947.
(41) Barguilla, I.; Domenech, J.; Ballesteros, S.; Rubio, L.; Marcos, R.; Hernández, A. Long-term exposure to nanoplastics alters molecular and functional traits related to the carcinogenic process. *J. Hazard. Mater.* **2022**, *438*, No. 129470.
(42) Domenech, J.; de Britto, M.; Velázquez, A.; Pastor, S.; Hernández, A.; Marcos, R.; Cortés, C. Long-Term Effects of Polystyrene Nanoplastics in Human Intestinal Caco-2 Cells. *Biomolecules* **2021**, *11*, No. 1142.
(43) Wagner, M.; Monclús, L.; Arp, H. P. H.; Groh, K. J.; Løseth, M. E.; Muncke, J.; Wang, Z.; Wolf, R.; Zimmermann, L. *State of the Science on Plastic Chemicals - Identifying and Addressing Chemicals and Polymers of Concern*; Zenodo, 2024.
(44) Martin, L. M. A.; Gan, N.; Wang, E.; Merrill, M.; Xu, W. Materials, surfaces, and interfacial phenomena in nanoplastics toxicology research. *Environ. Pollut.* **2022**, *292*, No. 118442.
(45) Luo, H.; Liu, C.; He, D.; Sun, J.; Li, J.; Pan, X. Effects of aging on environmental behavior of plastic additives: Migration, leaching, and ecotoxicity. *Sci. Total Environ.* **2022**, *849*, No. 157951.
(46) Shen, M.; Xiong, W.; Song, B.; Zhou, C.; Almatrafi, E.; Zeng, G.; Zhang, Y. Microplastics in landfill and leachate: Occurrence, environmental behavior and removal strategies. *Chemosphere* **2022**, *305*, No. 135325.
(47) Xu, D.; Ma, Y.; Peng, C.; Gan, Y.; Wang, Y.; Chen, Z.; Han, X.; Chen, Y. Differently surface-labeled polystyrene nanoplastics at an environmentally relevant concentration induced Crohn's ileitis-like features via triggering intestinal epithelial cell necroptosis. *Environ. Int.* **2023**, *176*, No. 107968.
(48) Lund, J.; Ouwens, D. M.; Wettergreen, M.; Bakke, S. S.; Thoresen, G. H.; Aas, V. Increased Glycolysis and Higher Lactate Production in Hyperglycemic Myotubes. *Cells* **2019**, *8*, No. 1101.
(49) da Justa Pinheiro, C. H.; Silveira, L. R.; Nachbar, R. T.; Vitzel, K. F.; Curi, R. Regulation of glycolysis and expression of glucose metabolism-related genes by reactive oxygen species in contracting skeletal muscle cells. *Free Radical Biol. Med.* **2010**, *48* (7), 953−960.
(50) Hidalgo, I. J.; Raub, T. J.; Borchardt, R. T. Characterization of the Human Colon Carcinoma Cell Line (Caco-2) as a Model System for Intestinal Epithelial Permeability. *Gastroenterology* **1989**, *96*, 736−749.
(51) Jeong, H.; Kim, W.; Choi, D.; Heo, J.; Han, U.; Jung, S. Y.; Park, H. H.; Hong, S.-T.; Park, J. H.; Hong, J. Potential threats of nanoplastic accumulation in human induced pluripotent stem cells. *Chem. Eng. J.* **2022**, *427*, No. 131841.
(52) Kalyanaraman, B.; Cheng, G.; Hardy, M.; Ouari, O.; Lopez, M.; Joseph, J.; Zielonka, J.; Dwinell, M. B. A review of the basics of mitochondrial bioenergetics, metabolism, and related signaling pathways in cancer cells: Therapeutic targeting of tumor mitochondria with lipophilic cationic compounds. *Redox Biol.* **2018**, *14*, 316−327.
(53) Mandal, S.; Lindgren, A. G.; Srivastava, A. S.; Clark, A. T.; Banerjee, U. Mitochondrial Function Controls Proliferation and Early Differentiation Potential of Embryonic Stem Cells. *Stem Cells* **2011**, *29* (3), 486−495.
(54) Rocheteau, P.; Chatre, L.; Briand, D.; Mebarki, M.; Jouvion, G.; Bardon, J.; Crochemore, C.; Serrani, P.; Lecci, P. P.; Latil, M.; Matot, B.; Carlier, P. G.; Latronico, N.; Huchet, C.; Lafoux, A.; Sharshar, T.; Ricchetti, M.; Chrétien, F. Sepsis induces long-term metabolic and mitochondrial muscle stem cell dysfunction amenable by mesenchymal stem cell therapy. *Nat. Commun.* **2015**, *6* (1), No. 10145.
(55) Hoffmann, R. F.; Zarrintan, S.; Brandenburg, S. M.; Kol, A.; de Bruin, H. G.; Jafari, S.; Dijk, F.; Kalicharan, D.; Kelders, M.; Gosker, H. R.; ten Hacken, N. H. T.; van der Want, J. J.; van Oosterhout, A. J. M.; Heijink, I. H. Prolonged cigarette smoke exposure alters mitochondrial structure and function in airway epithelial cells. *Respir. Res.* **2013**, *14* (1), No. 97.
(56) Huin, C.; Schohn, H.; Hatier, R.; Bentejac, M.; Antunes, L.; Plénat, F.; Bugaut, M.; Dauça, M. Expression of peroxisome proliferator-activated receptors alpha and gamma in differentiating human colon carcinoma Caco-2 cells. *Biol. Cell* **2002**, *94* (1), 15−27.
(57) Robine, S.; Huet, C.; Moll, R.; Sahuquillo-Merino, C.; Coudrier, E.; Zweibaum, A.; Louvard, D. Can villin be used to identify malignant and undifferentiated normal digestive epithelial cells? *Proc. Natl. Acad. Sci. U.S.A.* **1985**, *82* (24), 8488−8492.
(58) Endo, S.; Matsuoka, T.; Nishiyama, T.; Arai, Y.; Kashiwagi, H.; Abe, N.; Oyama, M.; Matsunaga, T.; Ikari, A. Flavonol glycosides of Rosa multiflora regulates intestinal barrier function through inhibiting claudin expression in differentiated Caco-2 cells. *Nutr. Res.* **2019**, *72*, 92−104.
(59) Ciana, A.; Meier, K.; Daum, N.; Gerbes, S.; Veith, M.; Lehr, C.-M.; Minetti, G. A dynamic ratio of the α+ and α− isoforms of the tight junction protein ZO-1 is characteristic of Caco-2 cells and correlates with their degree of differentiation. *Cell Biol. Int.* **2010**, *34* (6), 669−678.

https://doi.org/10.1021/acs.est.3c10868
Environ. Sci. Technol. 2024, 58, 9967−9979

(60) Briske-Anderson, M. J.; Finley, J. W.; Newman, S. M. The Influence of Culture Time and Passage Number on the Morphological and Physiological Development of Caco-2 Cells. *Exp. Biol. Med.* **1997**, *214* (3), 248−257.
(61) Seo, B. J.; Yoon, S. H.; Do, J. T. Mitochondrial Dynamics in Stem Cells and Differentiation. *Int. J. Mol. Sci.* **2018**, *19*, No. 3893.

https://doi.org/10.1021/acs.est.3c10868
Environ. Sci. Technol. 2024, 58, 9967−9979